Supplementary Information

Interplay between Near-Field Properties and Au Nanorod Cluster Structure: Extending Hot Spots for Surface-Enhanced Raman Scattering

Klester S. Souza,[a,b] Erico Teixeira-Neto,[c] Marcia L. A. Temperini*[a] and Diego P. dos Santos*[,d]

[a]*Departamento de Química Fundamental, Universidade de São Paulo, 05508-000 São Paulo-SP, Brazil*

[b]*Departamento de Química Inorgânica, Instituto de Química, Universidade Federal do Rio Grande do Sul, 91501-970 Porto Alegre-RS, Brazil*

[c]*Departamento de Química Inorgânica, Instituto de Química, Universidade Estadual de Campinas, 13083-970 Campinas-SP, Brazil*

[d]*Departamento de Físico-Química, Instituto de Química, Universidade Estadual de Campinas, 13083-970 Campinas-SP, Brazil*

*e-mail: santosdp@unicamp.br; mlatempe@iq.usp.br

Surface-enhanced Raman scattering (SERS)-transmission electron microscopy (TEM) correlation

Figure S1 shows a scheme of the experimental procedure to obtain the correlation between SERS and Au nanorods (NR) clusters. Small AuNRs clusters are not visible by optical microscopy Figures S1A and S1B. SERS mappings where performed along a line (as indicated in the figure) with 1 μm step between each analysis, when a SERS signal was observed, the corresponding region was analyzed by transmission electron microscopy searching for the aggregates responsible for the SERS signal. The SERS mapping was obtained in delimited regions on the substrate, (i.e., regions chosen where visible large aggregates or surface defects were observed by the Raman optical microscope in the Raman instrument); then in the electron transmission microscope those same regions were latter analyzed to investigate the structures of the AuNRs clusters. The correlations (SERS - AuNRs cluster morphology) of interest were those in which we had the presence of only one AuNRs cluster in the analyzed area. In this case we have great confidence that only one nanostructure contributes to the obtained SERS spectra.

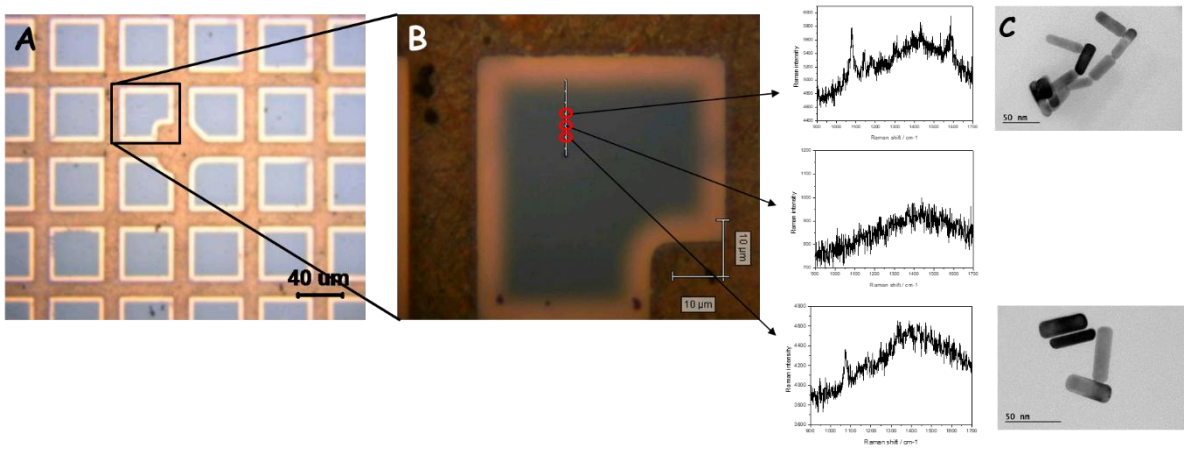

Figure S1. Scheme of the experimental procedure to obtain the correlation between SERS and AuNRs cluster morphology. (A) Optical image of the carbon grid, after deposition of AuNRs, (B) region where SERS mapping where performed, and the obtained spectra. (C) Transmission electron microscopy images of the aggregates in the region of the SERS mapping.

Grid size effect on discrete dipole approximation (DDA) simulations

Figure S2 shows the effect of changing the grid spacing in the DDA simulations from 0.25 to 0.5 nm.

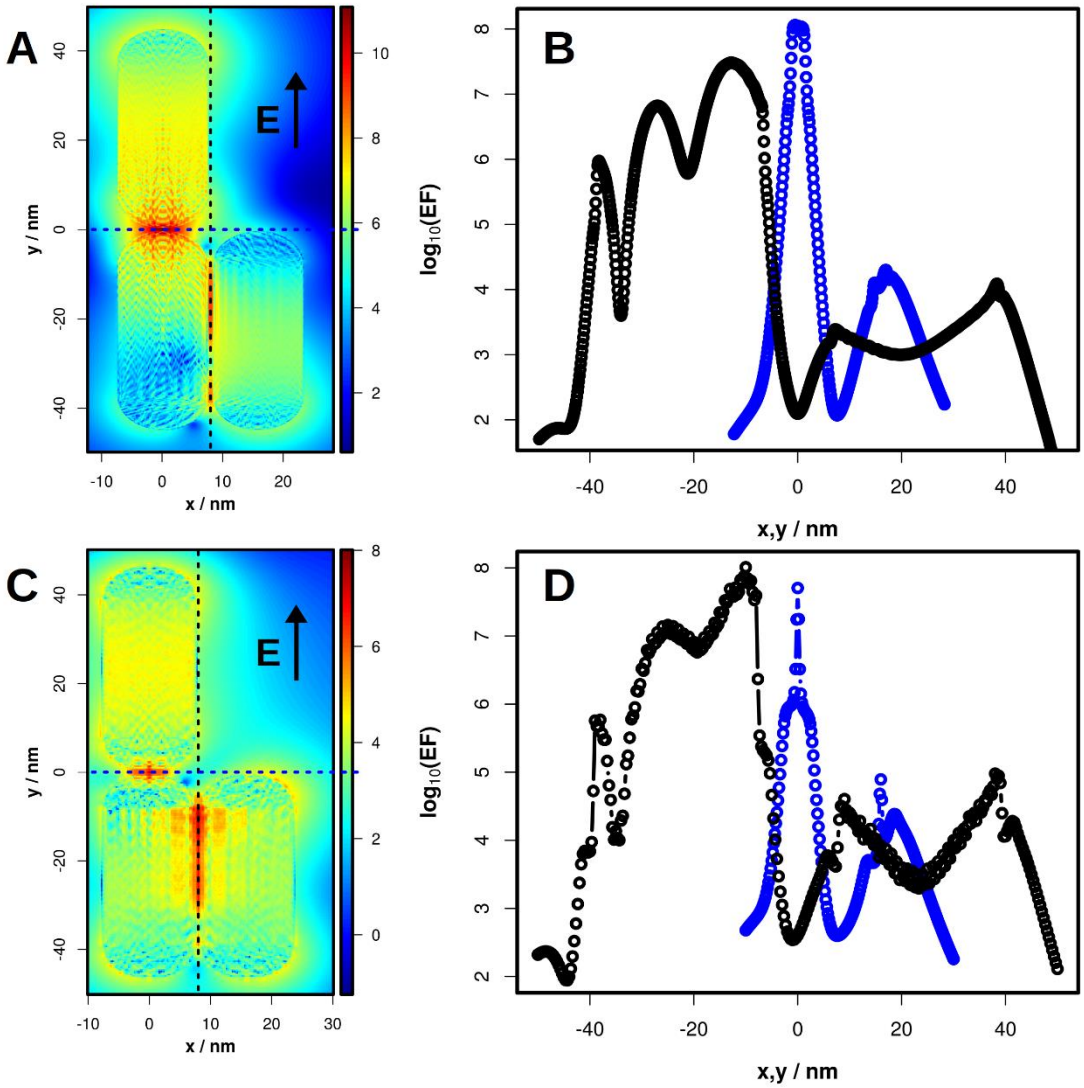

Figure S2. Comparison of DDA enhancement factors (EF) simulations for the asymmetric trimer illuminated with a plane wave with polarization along the AuNRs long axis and wavelength 662 nm. (A) and (B) show the results for grid spacing equals to 0.25 nm, whereas (C) and (D) show the results for 0.5 nm spacing. (B) and (D) show the EF profiles along the dashed lines indicated in the maps.

As it can be seen in Figure S2, a good qualitative agreement between the field distributions can be observed for simulations with resolutions 0.25 nm (Figures S2A and S2B) and 0.5 nm (Figures S2C and S2D). Both resolutions are able to describe both the ee and ss hot spot regions and their field behaviors. As expected, the spatial dependence of the EF profile in the ee hot spot for 0.5 nm (Figure S2D) is not as accurate as for 0.25 nm resolution (Figure S2B) and this is due to the very fast decay of fields in such regions. Nevertheless, the overall result of asymmetric AuNRs cluster structures is depicted in both simulations. Therefore, the above results suggest that we can use the lower resolution for larger clusters without much prejudice in the analysis.

Boundary element method (BEM) simulations

Figure S3 presents retarded BEM simulations of the model asymmetric trimer for incident light electric field polarization along the AuNR longitudinal axis (black) and along the transversal axis (red).

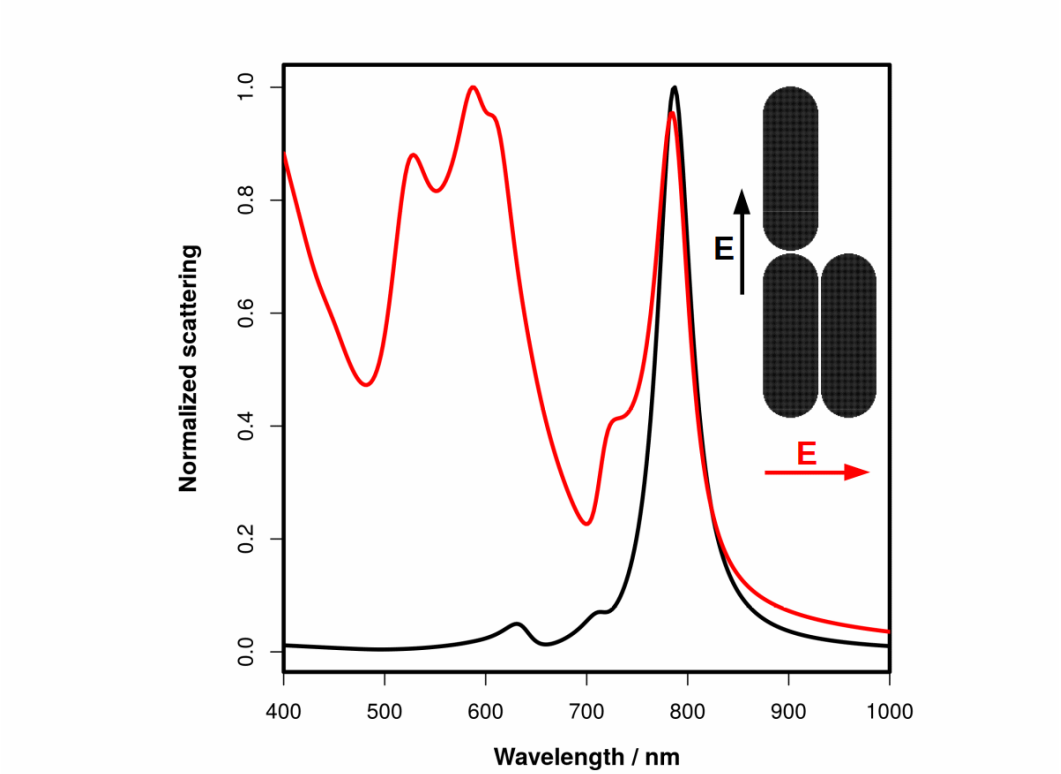

Figure S3. BEM simulations for the AuNR model trimer for two different incident light electric field polarizations.

The BEM scattering spectrum for polarization along the longitudinal AuNR axis shows a strong correlation with the DDA simulated spectrum. This correspondence makes possible the analysis of the modes through the BEM surface charge distributions. It is also presented in Figure S3 the scattering spectrum for orthogonal polarization, i.e., along the transversal axis of the AuNR (red). It is interesting to note that even for such polarization it can be observed the mode at 796 nm, which according to our coupled oscillator analysis has a great contribution of a ee mode. Also, for such polarization it can be observed higher energy modes that can be interpreted as single AuNR transversal mode and to a dipolar coupling of such transversal mode in the ss arrangement.

Figure S4 shows the BEM surface charges for different light wavelength excitation.

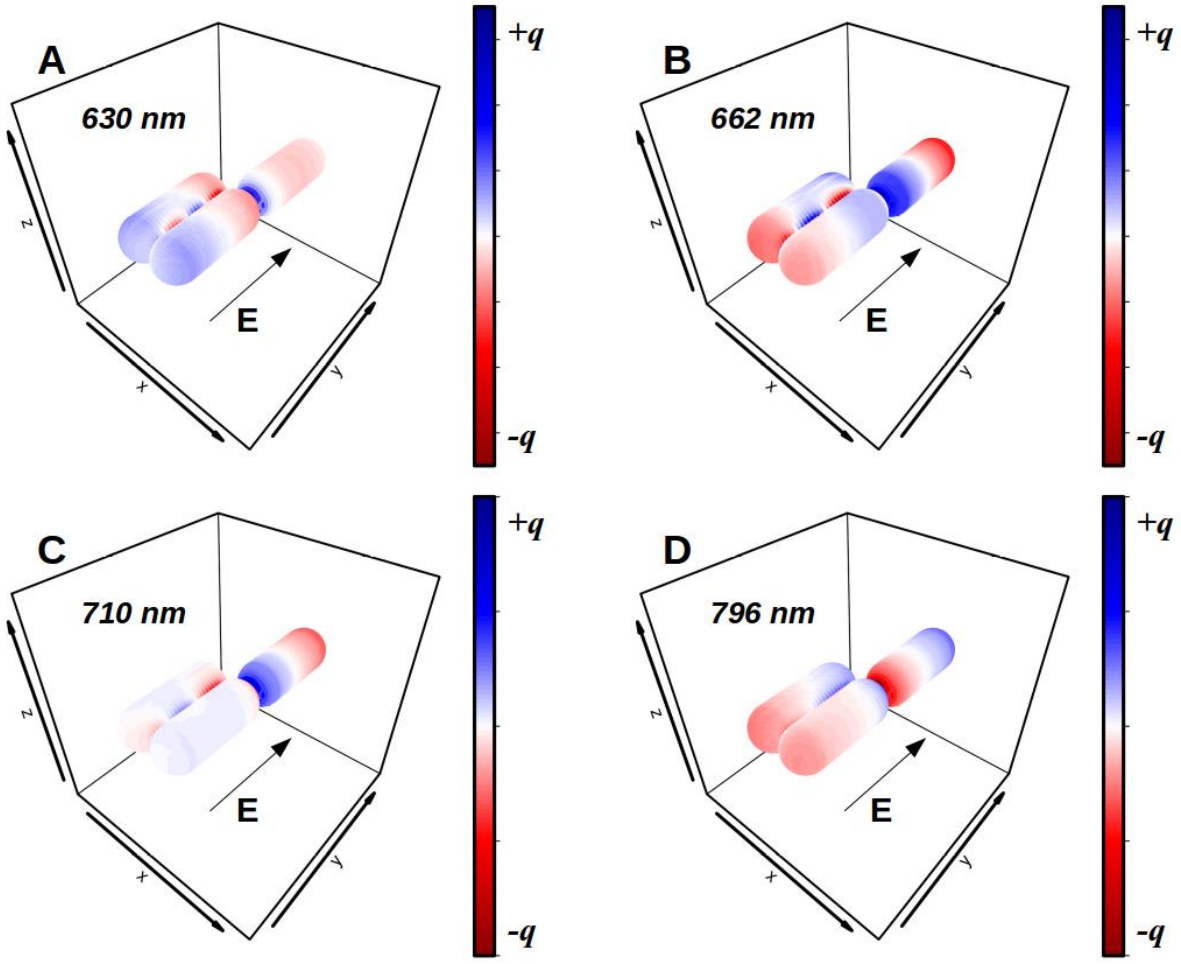

Figure S4. BEM surface charges for different incident light wavelengths. The blue and red colors refer to positive and negative charge densities.

The surface charge densities of Figure S4 show a good correspondence with the interpretation from the coupled oscillator analysis. For instance, the mode at 710 nm shows a charge density distribution mainly deposited as a dipolar plasmon mode of an individual AuNR. Whereas, at 630 nm, the contribution of this single AuNR is smaller and the contribution associated to an *ss* dimer is considerably greater. Note that at 662 nm (Fano dip) it is possible to observe the contribution from both single AuNR as well as *ss* dimer. Also, these two modes appear to be out-of-phase, consistent with the Fano interference. For 796 nm all three particles appear to contribute to the mode, consistent with the in-phase coupling between a single particle mode with the ee dimer mode.

Incident polarization effects on the SERS enhancement factor (EF) distributions

Figures S5 and S6 show SERS EF maps for incident electric field polarization along the *x* axis in the figure, i.e., along the AuNR transversal axis.

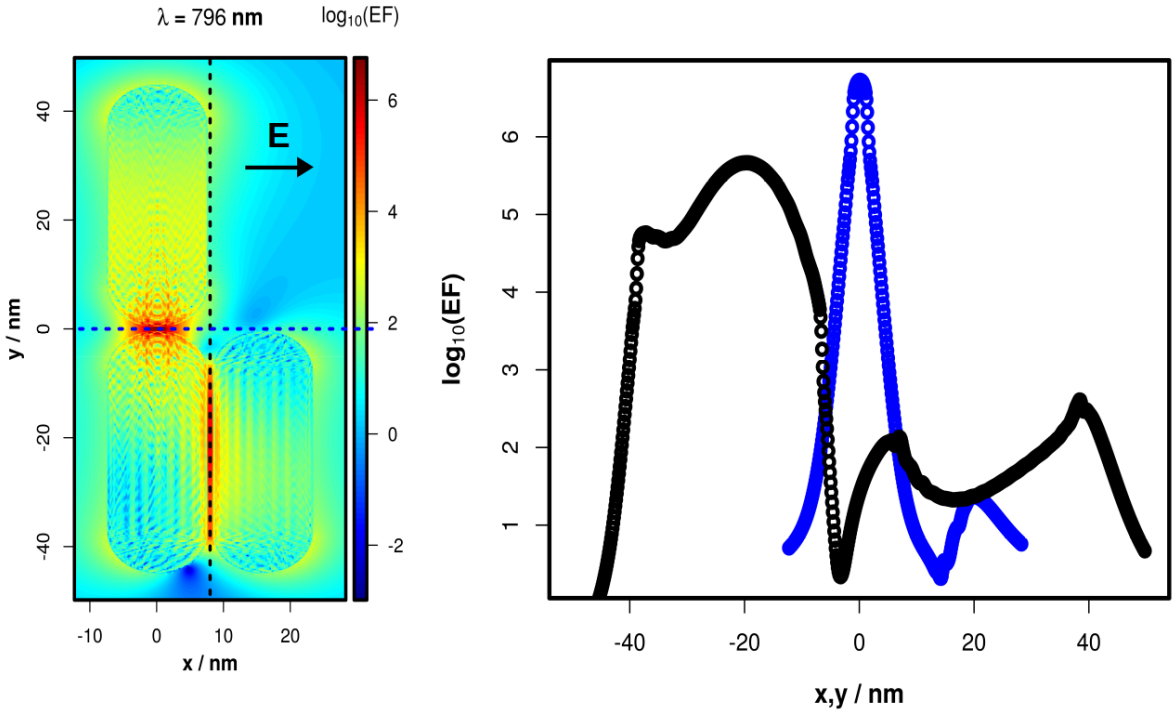

Figure S5. (A) SERS EF 2D map for incident excitation polarization along the AuNR transversal axis (along the *x* axis in the figure). (B) $\log_{10}$(EF) along the black and blue dashed lines (along *x* and *y* axis respectively). The simulation was performed for incident light wavelength at 796 nm.

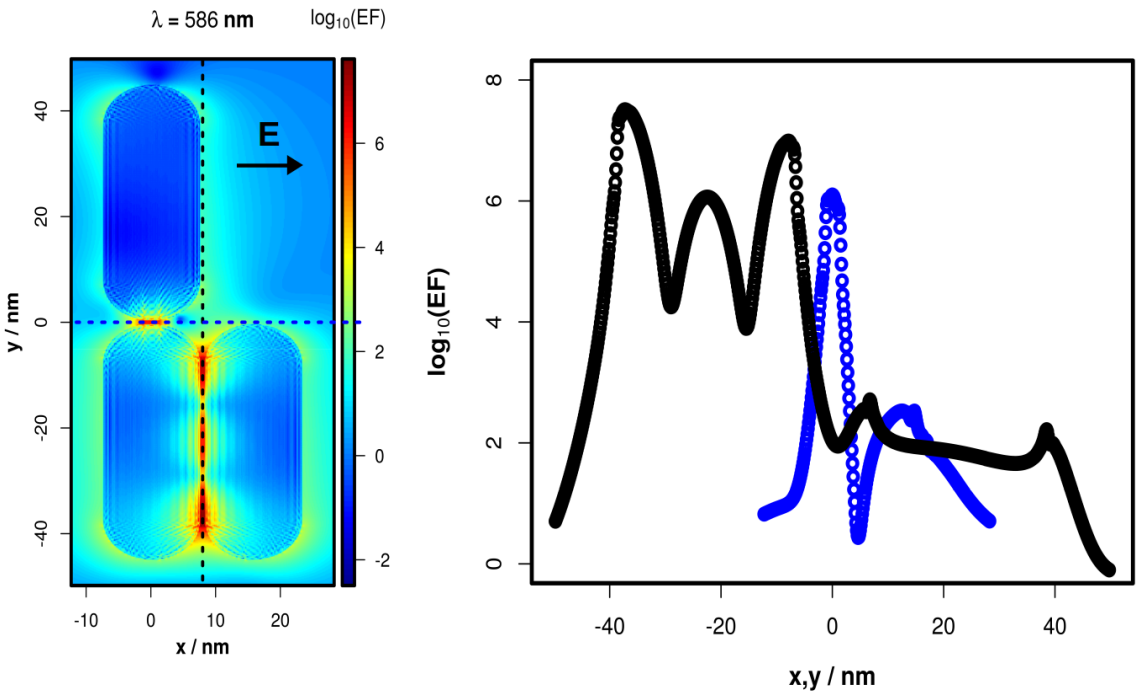

Figure S6. (A) SERS EF 2D map for incident excitation polarization along the AuNR transversal axis (along the *x* axis in the figure). (B) log10(EF) along the black and blue dashed lines (along *x* and *y* axis respectively). The simulation was performed for incident light wavelength at 586 nm.

For polarization along the AuNR transversal axis, it can also be observed strong field enhancements in the hot spot formed between ss arranged particles, especially for excitation at 586 nm, which is associated to the dipolar coupling between transversal plasmon modes in such configuration. It is interesting to see that the maximum enhancement in these regions is larger at this excitation than at 796 nm for the same polarization. Also, it can be observed a great degree of fluctuation of EFs in the ss hot spot for 586 nm than for 796 nm. However, as expected, the larger EF in the ee hot spot is observed for 796 nm. Nevertheless, the enhancements observed in such simulations are smaller than the observed for longitudinal polarization (i.e., along the *y* axis in the figure) and 796 nm wavelength excitation. This is another indication that the differential behavior observed for asymmetric AuNR clusters are related to ee hot spot polarization.